New Version of the Rayleigh–Schrödinger Perturbation Theory: Examples

MILOŠ KALHOUS,[1] L. SKÁLA,[1] J. ZAMASTIL,[1] J. ČÍŽEK[2]

[1]*Charles University, Faculty of Mathematics and Physics, Ke Karlovu 3, 12116 Prague 2, Czech Republic*

[2]*University of Waterloo, Waterloo, Ontario N2L 3G1, Canada*

Received 22 January 2003; accepted 10 October 2003
Published online 9 June 2004 in Wiley InterScience (www.interscience.wiley.com).
DOI 10.1002/qua.20041

ABSTRACT: It has been shown in our preceding papers that the linear dependence of the perturbation wave functions on the perturbation energies makes possible to calculate the exact perturbation energies from the values of the perturbation wave functions corresponding to arbitrarily chosen trial perturbation energies. The resulting version of the perturbation theory is very simple and can be used at large orders. In this paper, this method is applied to a few problems and its numerical properties are discussed. Int J Quantum Chem 99: 325–335, 2004

1. Introduction

In this paper, we are interested in the perturbation theory for the bound states of the Schrödinger equation:

$$H\psi(x) = E\psi(x). \tag{1}$$

As usual in the Rayleigh–Schrödinger perturbation theory, we assume the Hamiltonian, wave function, and energy to be in the forms

$$H = H_0 + \lambda H_1, \tag{2}$$

$$\psi = \psi_0 + \lambda\psi_1 + \lambda^2\psi_2 + \cdots, \tag{3}$$

$$E = E_0 + \lambda E_1 + \lambda^2 E_2 + \cdots, \tag{4}$$

where λ is a perturbation parameter. Using these assumptions in the Schrödinger equation (1), we obtain the well-known equations for E_n and ψ_n,

$$H_0\psi_0 = E_0\psi_0 \tag{5}$$

and

$$H_0\psi_n + H_1\psi_{n-1} = \sum_{i=0}^{n} E_i\psi_{n-i},\ n = 1, 2, \ldots. \tag{6}$$

Correspondence to: L. Skála; e-mail: skala@karlov.mff.cuni.cz

We note that ψ_0 denotes the unperturbed wave function of the Hamiltonian H_0. Depending on the problem in question, it can be the ground-state as well as excited-state wave function.

Despite the well-known formulations that can be found in any textbook on quantum mechanics, there is one property of the perturbation theory that has been noticed [1, 2] and used [3–9] only recently. It has been shown that the value of the perturbation wave function $\psi_n(x)$ at an arbitrarily chosen point x depends linearly on the perturbation energy E_n. This linear dependence makes it possible to determine the exact perturbation energies from the values of $\psi_n(x)$ for two arbitrarily chosen trial perturbation energies E_n by simple calculation. In this way, the functions ψ_n which are not quadratically integrable can be used to calculate the exact perturbation energies E_n and, in the next step, the corresponding exact perturbation functions ψ_n.

This method has a few advantages. In contrast to the usual formulation of the perturbation theory, this method based on the computation of ψ_n from Eq. (6) for a given energy E_n can easily be programmed for arbitrary large orders of the perturbation theory. For example, 200 perturbation energies E_n necessary for finding their large-order behaviour were calculated in [7]. Further, by solving Eq. (6) numerically, both the discrete and the continuous parts of the energy spectrum is taken into account, and the perturbation energies E_n can be calculated even in cases when only a few bound states exist. The linear dependence of $\psi_n(x)$ on the energy E_n makes it possible to avoid the usual shooting method and reduce the computational time substantially. Finally, we note that only the wave functions are needed in this method and no integrals have to be calculated.

The aim of this paper is to apply this method to a few problems and test its numerical properties.

2. Summary of the Method

First we discuss a nondegenerate multidimensional case. We assume that the perturbation functions ψ_i and perturbation energies E_i are already computed for $i = 0, \ldots, n-1$. Solution of Eq. (6) can be written as

$$\psi_n(E_n, x) = E_n F(x) - f_{n-1}(x), \; n = 1, 2, \ldots, \quad (7)$$

where

$$F(x) = (H_0 - E_0)^{-1}\psi_0(x) \quad (8)$$

and

$$f_{n-1}(x) = (H_0 - E_0)^{-1}\left(H_1\psi_{n-1}(x) - \sum_{i=1}^{n-1} E_i\psi_{n-i}(x) \right). \quad (9)$$

The general solution of Eq. (6) can contain also a term $c_n\psi_0(x)$ at the right-hand side of Eq. (7), where c_n is an arbitrary constant. For the sake of simplicity, we assume $c_n = 0$ here. As it is seen from Eq. (7), the perturbation function $\psi_n(E_n, x)$ depends on the energy E_n which is not yet known and the point $x = [x_1, \ldots, x_N]$ in N-dimensional space.

Equations (7)–(9) show that the structure of the perturbation functions is very simple. It follows from Eq. (7) that the function $\psi_n(E_n, x)$ is a *linear function* of the energy E_n. Further, it is seen that $F(x)$ is a function *independent* of n. We note also that, except for the case that E_n is the exact perturbation energy, $\psi_n(E_n, x)$ is not quadratically integrable and has no physical meaning.

The functions $F(x)$ and $f_{n-1}(x)$ are calculated from Eqs. (8) and (9) numerically with the conditions $F(x_b) = 0$ and $f_{n-1}(x_b) = 0$, where x_b are points at the boundary region sufficiently distant from the potential minimum. The same boundary conditions are used for the function $\psi_0(x)$.

We note that the function $F(x)$ diverges in the exact calculation, however, it has large but finite values in numerical calculations. The functions $\psi_n(E_n, x)$ for the exact perturbation energy E_n are quadratically integrable. Therefore, we can assume they obey the condition

$$|\psi_n(E_n, x)| \ll |F(x)|. \quad (10)$$

It follows from Eqs. (7) and (10) that the functions $\psi_n(E_n, x)$ also satisfy the condition

$$|\psi_n(E_n, x)| \ll |f_{n-1}(x)|. \quad (11)$$

Therefore, we can neglect $\psi_n(E_n, x)$ in Eq. (7). The formula for the energy E_n then reads

$$E_n = \frac{f_{n-1}(x)}{F(x)}. \quad (12)$$

This equation can be used at an *arbitrarily chosen point* x inside the integration region except for the

points where the conditions (10) and (11) are not obeyed.

If the perturbation energy E_n is calculated from Eq. (12), the corresponding perturbation function $\psi_n(E_n, x)$ can be found from Eqs. (7)–(9). More detailed discussion of the method is given in [6, 9].

The energy E_1 computed numerically from the equation

$$E_1(x_0) = \frac{f_0(x_0)}{F(x_0)} \tag{13}$$

depends slightly on the choice of the point x_0. Calculating ψ_1 from Eq. (7) for $n = 1$, we obtain the function

$$\psi_1(E_1, x) = \frac{f_0(x_0)\,F(x) - f_0(x)\,F(x_0)}{F(x_0)}. \tag{14}$$

It shows that the function ψ_1 calculated in this way equals zero at the point x_0:

$$\psi_1(E_1, x_0) = 0. \tag{15}$$

Therefore, the usual orthogonality condition, $\langle\psi_0|\psi_1\rangle = 0$, is not fulfilled in numerical calculations. It can easily be shown that this result can be extended to all functions ψ_n. As shown in [6], such functions can have in some cases more simple form than the usual perturbation functions. If necessary, the functions ψ_n can be made orthogonal to ψ_0 by the usual orthogonalization procedure.

Therefore, the point x used in the calculation of the energy (12) should be sufficiently distant from the points where the function $\psi_0(x)$ equals zero.

Our method is a remarkable example of calculating the perturbation energies E_n from the values of the functions $F(x)$ and $f_{n-1}(x)$ which are not quadratically integrable. Comparing with the standard formulation of the perturbation theory, large-order calculations are simple in our method. To determine E_1, the values of $F(x)$ and $f_0(x)$ at only one point x are sufficient. To determine E_n for $n = 2, 3, \ldots,$ only the value of $f_{n-1}(x)$ at the point x is to be computed. Therefore, this method of calculating E_n is much faster than the usual shooting method.

We note that the zero-order function ψ_0 has to be found only for the state for which the perturbation corrections are calculated. In contrast to the usual perturbation theory, other zero-order energies and wave functions are not needed in the calculation.

Now we discuss the first-order perturbation correction to a degenerate eigenvalue E_0. Assuming that the energy E_0 is d_0-times degenerate and the corresponding zero-order function ψ_0 in Eq. (6) is replaced by the linear combination

$$\sum_{j=1}^{d_0} a_0^{(j)}\psi_0^{(j)}, \tag{16}$$

it follows from Eq. (6) that Eq. (7) can be generalized as

$$\psi_1(E_1, x) = E_1 \sum_{j=1}^{d_0} a_0^{(j)}F^{(j)}(x) - \sum_{j=1}^{d_0} a_0^{(j)}f_0^{(j)}(x), \tag{17}$$

where

$$F^{(j)}(x) = (H_0 - E_0)^{-1}\psi_0^{(j)}(x) \tag{18}$$

and

$$f_0^{(j)}(x) = (H_0 - E_0)^{-1}H_1\psi_0^{(j)}(x). \tag{19}$$

It is seen from Eq. (17) that $\psi_1(E_1, x)$ depends on E_1 linearly as in the nondegenerate case. Therefore, by analogy with the nondegenerate case, we can derive the formula for the perturbation energy E_1:

$$E_1 = \frac{\sum_{j=1}^{d_0} a_0^{(j)}f_0^{(j)}(x)}{\sum_{j=1}^{d_0} a_0^{(j)}F^{(j)}(x)}. \tag{20}$$

Here, $f_0^{(j)}(x)$ and $F^{(j)}(x)$ are known, and E_1 and $a_0^{(j)}$ are to be found. To find E_1 and $a_0^{(j)}$, we exploit the fact that the energy E_1 is a constant and use Eq. (20) at d_0 different points $x = x_1, \ldots, x_{d_0}$ inside the integration region. The solution of the equations

$$\frac{\sum_{j=1}^{d_0} a_0^{(j)}f_0^{(j)}(x_1)}{\sum_{j=1}^{d_0} a_0^{(j)}F^{(j)}(x_1)} = \frac{\sum_{j=1}^{d_0} a_0^{(j)}f_0^{(j)}(x_2)}{\sum_{j=1}^{d_0} a_0^{(j)}F^{(j)}(x_2)} = \cdots = \frac{\sum_{j=1}^{d_0} a_0^{(j)}f_0^{(j)}(x_{d_0})}{\sum_{j=1}^{d_0} a_0^{(j)}F^{(j)}(x_{d_0})} \tag{21}$$

then yields d_0 sets of the coefficients $a_0^{(j)}$. The d_0 values of the energy E_1 are given by Eq. (20), and the corresponding perturbation functions equal

$$\psi_1 = \sum_{j=1}^{d_0} a_0^{(j)}\psi_0^{(j)}. \tag{22}$$

The usual formulation of the first-order degenerate perturbation theory can be derived from Eq. (20) as follows. Substitute Eqs. (18) and (19) into Eq. (20), and we obtain for a point x

$$E_1 = \frac{\sum_{j=1}^{d_0} a_0^{(j)}(H_0 - E_0)^{-1}H_1\psi_0^{(j)}(x)}{\sum_{j=1}^{d_0} a_0^{(j)}(H_0 - E_0)^{-1}\psi_0^{(j)}(x)}. \quad (23)$$

By multiplying the numerator and denominator by $(H_0 - E_0)$, we obtain

$$E_1 = \frac{\sum_{j=1}^{d_0} a_0^{(j)}H_1\psi_0^{(j)}(x)}{\sum_{j=1}^{d_0} a_0^{(j)}\psi_0^{(j)}(x)} \quad (24)$$

and

$$E_1 \sum_{j=1}^{d_0} a_0^{(j)}\psi_0^{(j)}(x) = \sum_{j=1}^{d_0} a_0^{(j)}H_1\psi_0^{(j)}(x). \quad (25)$$

Further, by multiplying this equation from the left side by the complex conjugate function $\psi_0^{(i)*}(x)$, integrating over x, and assuming orthonormality of the functions $\psi_0^{(j)}(x)$, a standard secular problem is obtained:

$$\sum_{j=1}^{d_0} (W_{ij} - E_1\delta_{ij})a_0^{(j)} = 0,\ i = 1, \ldots, d_0, \quad (26)$$

where

$$W_{ij} = \langle\psi_0^{(i)}|H_1|\psi_0^{(j)}\rangle. \quad (27)$$

3. Examples

For the one-dimensional problems, this method has already been used with very good results (see [3–8]). For this reason, several two-dimensional problems with increasing complexity are investigated here.

3.1. COUPLED ANHARMONIC OSCILLATORS

As the first example, we discuss the problem having only bound discrete states. We calculated the perturbation energies for the ground state of two nonlinearly coupled harmonic oscillators [9–11]:

TABLE I

Perturbation energies E_n for the ground state of two coupled harmonic oscillators (28); E_0 is the exact zero-order energy.

n	E_n
0	2
1	−0.750000000
2	−0.93750000
3	−0.0234375000
4	−0.0133056640
5	−0.00031534830
6	−0.013279491
7	0.0240443106
8	−0.0743030687
9	0.234920366
10	−0.84554255
11	3.34568731
12	−14.4946548
13	68.195859
14	−346.32541
15	1888.18252
16	−11000.3994
17	68201.932
18	−448367.10
19	3115424.0
20	−22813412.6

$$H = -\frac{\partial^2}{\partial x_1^2} - \frac{\partial^2}{\partial x_2^2} + x_1^2 + x_2^2 + \lambda(x_1^2x_2^2 - x_1^2 - x_2^2). \quad (28)$$

To compute ψ_n from Eq. (6) in the region $x_1 \in [-11, 11]$, $x_2 \in [-11, 11]$, we used a grid of points 158×158, 160×160, 162×162, 164×164, assumed that the functions ψ_n equal zero at the border of this region, and solved the corresponding system of difference equations in double-precision accuracy in Fortran. The same grid of points was used in all examples given below, only the integration region was different.

To eliminate the effect of a non-zero step of the grid the perturbation energies were extrapolated to an infinitely dense grid by means of the Richardson extrapolation. This extrapolation is substantial for increasing the accuracy of the results. The ground-state perturbation energies are shown in Table I.

Only the digits which agree in the calculations for the points $x = [0, 0]$ and $x = [1, 1]$ are shown. It is seen that the energies depend on the choice of the point x only very little. All digits shown in Table I also agree with an independent calculation made

TABLE II

Perturbation energies E_n for the ground state of two coupled Morse oscillators (29); E_0 is the exact zero-order energy.

n	E_n
0	3/2
1	0.2500000
2	−0.069635
3	0.03903
4	−0.0366
5	0.0920
6	−0.611
7	6.43
8	−89.2
9	1550

by means of the difference equation method suggested in [11]. It is also seen that the method can be used at large orders. Therefore, these results are quite satisfactory.

3.2. COUPLED MORSE OSCILLATORS

As a second test, we chose a more difficult problem with only one bound state of the zero-order Hamiltonian when the standard perturbation theory yields the first-order correction E_1 only. The perturbation energies were calculated for the ground state of two coupled Morse oscillators:

$$H = -\frac{\partial^2}{\partial x_1^2} - \frac{\partial^2}{\partial x_2^2} + (1 - e^{-x_1})^2 + (1 - e^{-x_2})^2 + \lambda(1 - e^{-x_1})^2(1 - e^{-x_2})^2. \quad (29)$$

The integration region $x_1 \in [-12, 20]$ and $x_2 \in [-12, 20]$ was used. The ground-state perturbation energies are shown in Table II.

Only the digits that agree in the calculations for the points $x = [4, 4]$ and $x = [5, 6]$ are shown. The value of $E_1 = 0.25$ was verified by analytic calculation. Decreasing accuracy of the energies E_n with increasing n is due to the fact that the functions ψ_n spread with increasing n rapidly and get out of the integration region. These results show that, in contrast to the standard perturbation theory, our method can be used for calculating large-order perturbation energies even if there are only a few zero-order bound states.

3.3. BARBANIS HAMILTONIAN

As another example of using our method we calculated the perturbation energies for the ground state of the Barbanis Hamiltonian:

$$H = -\frac{\partial^2}{\partial x^2} - \frac{\partial^2}{\partial y^2} + \omega_x^2 x^2 + \omega_y^2 y^2 + \lambda x y^2. \quad (30)$$

Here, we used the frequencies $\omega_x = 1$ and $\omega_y = 1$. This Hamiltonian has been often studied as a simple model for systems with the Fermi responses such as the CO_2 stretch bend resonance. Potential in this Hamiltonian is not bounded from below.

The ground-state perturbation energies were calculated both numerically and analytically (see Table III).

In the numerical calculation, the integration region $x \in [-11, 11]$ and $y \in [-11, 11]$ was used. Similarly to the preceding examples, only the digits that agree in the calculations for the points $x = [0.2, 0.5]$ and $x = [0.6, 0.8]$ are shown. Again, the energies depend on the choice of the point x only little. The numerical results agree with an independent analytic calculation made in Maple [12] with an accuracy to 6–9 digits. Due to the antisymmetry of the perturbation potential in Eq. (30), the odd-order perturbation energies $E_1, E_3, \ldots$ equal zero.

3.4. HÉNON-HEILES HAMILTONIAN

As the last test of our method, the Hénon–Heiles Hamiltonian was used. The perturbation energies were calculated for the ground state and the first excited state of the zero-order Hamiltonian

$$H_0 = -\frac{1}{2}\frac{\partial^2}{\partial x^2} + \frac{1}{2}\omega_x^2 x^2 - \frac{1}{2}\frac{\partial^2}{\partial y^2} + \frac{1}{2}\omega_y^2 y^2 \quad (31)$$

with the perturbation potential

$$H_1 = y x^2 + \beta y^3. \quad (32)$$

The frequencies $\omega_x = 2$, $\omega_y = 1.3$, and the parameter $\beta = -1$ corresponding to a very flat and shallow potential minimum were used. Similarly to the Barbanis potential, the perturbation potential is not bounded from below.

The analytic energies and wave functions of the Hénon–Heiles potential can be calculated as follows.

First, we express the eigenfunctions of H_0 as the products of the eigenfunctions of the harmonic os-

TABLE III

Perturbation energies E_n for the ground state of the Barbanis Hamiltonian (30); E_0 is the exact zero-order energy.*

n	E_n^{num}	E_n^{an}
0	2	2
2	−0.1041666665	$-\frac{5}{48} = -0.104166666667\ldots$
4	−0.0322627314	$-\frac{223}{6912} = -0.0322627314815\ldots$
6	−0.02298880368	$-\frac{114407}{4976640} = -0.0229888036908\ldots$
8	−0.024159131	$-\frac{346266143}{14332723200} = -0.0241591313924\ldots$
10	−0.0326818070	$-\frac{2360833242959}{72236924928000} = -0.0326818070580\ldots$
12	−0.05343610684	$-\frac{12969801730008377}{242716067758080000} = -0.0534361068462\ldots$
14	−0.1019221649	$-\frac{12468026134627585849 1}{122328898150072320000 0} = -0.101922164944\ldots$
16	−0.2217101989	$-\frac{10935414749213048671720261}{49323011734109159424000000} = -0.221710199048\ldots$
18	−0.541404172	$-\frac{444135678263749975690598035 1899}{820340331161703539539968000000 0} = -0.541404172625\ldots$
20	−1.46666250	$-\frac{667033238517271928733626515967166703}{454796679596048442320958259200000000} = -1.46666250754\ldots$
22	−4.366576807	
24	−14.17768870	
26	−49.8757770	
28	−189.0381799	
30	−768.15366	

* The energies calculated numerically from Eq. (12) are denoted as E_n^{num}. The analytic energies denoted as E_n^{an} were calculated for $n = 0, 2, \ldots, 20$. Odd-order perturbation energies equal zero.

cillator. For example, the ground-state zero-order wave function equals

$$\varphi_{00}(x, y) = \frac{1}{5\sqrt{\pi}}\, 13^{1/4}5^{3/4}e^{-x^2-(13/20)y^2} = \varphi_0(x)\varphi_0(y). \quad (33)$$

Analogously, orthonormal excited state wave functions corresponding to low quantum numbers can be written in the form

$$\varphi_{01}(x, y) = \frac{1}{5\sqrt{\pi}}\, 13^{3/4}5^{1/4}ye^{-x^2-(13/20)y^2} = \varphi_0(x)\varphi_1(y), \quad (34)$$

$$\varphi_{03}(x, y) = \frac{\sqrt{6}}{150\sqrt{\pi}}\, 13^{3/4}5^{1/4}y(-15 + 13y^2)e^{-x^2-(13/20)y^2} = \varphi_0(x)\varphi_3(y), \quad (35)$$

and

$$\varphi_{21}(x, y) = \frac{\sqrt{2}}{10\sqrt{\pi}}\, 13^{3/4}5^{1/4}(-1 + 4x^2)ye^{-x^2-(13/20)y^2} = \varphi_2(x)\varphi_1(y). \quad (36)$$

Now we discuss the ground-state perturbation problem with the zero-order wave function

$$\psi_0(x, y) = \varphi_{00}(x, y). \tag{37}$$

After a simple but tedious calculation, $H_1\psi_0$ can be expressed as a linear combination of the eigenfunctions of the unperturbed Hamiltonian H_0:

$$H_1\psi_0 = -\frac{47\sqrt{65}}{676}\varphi_{01} - \frac{5\sqrt{390}}{169}\varphi_{03} - \frac{\sqrt{130}}{52}\varphi_{21}. \tag{38}$$

The first-order perturbation energy equals zero:

$$E_1 = \langle\psi_0|H_1|\psi_0\rangle = 0. \tag{39}$$

The corresponding eigenfunction can be calculated from the equation

$$\psi_1 = (H_0 - E_0)^{-1}(E_1 - H_1)\psi_0, \tag{40}$$

with the result

$$\psi_1 = -\frac{2}{26871}\frac{1}{\sqrt{\pi}}13^{1/4}5^{3/4}y(-1200 - 689y^2 + 507x^2)e^{-x^2-(13/20)y^2}. \tag{41}$$

Higher order perturbation energies and wave functions can be obtained in a similar way. For example, the second- and third-order perturbation wave functions equal

$$\psi_2 = \frac{5}{6608207466432}\frac{1}{\sqrt{\pi}}13^{1/4}5^{3/4}(-59250448263 + 94848624000y^2 + 45306655680y^4 + 8689293184y^6 - 5426185752x^2 - 25233511680x^2y^2 - 12788016384x^2y^4 + 588128112x^4 + 4705024896x^4y^2)e^{-x^2-(13/20)y^2} \tag{42}$$

and

$$\psi_3 = -\frac{25}{652300246187820708192}\frac{1}{\sqrt{\pi}}13^{1/4}5^{3/4}y(-267842001350803600 - 1402374103429392171y^2 - 753269605832315520y^4 - 152737767077163840y^6 - 14661974436247424y^8 - 63207691842935367x^2 + 441043571586179016x^2y^2 + 183753938493178560x^2y^4 + 32367000170583936x^2y^6 - 25884928192802328x^4 - 55488811253153616x^4y^2 - 23817226540618368x^4y^4 + 2190735460104048x^6 + 5841961226944128x^6y^2)e^{-x^2-(13/20)y^2}. \tag{43}$$

These functions agree very well with the numerically calculated ones and are shown in Figures 1–4.

It is seen that the ground-state perturbation functions go to zero at the boundaries of the integration region $x \in [-11, 11]$ and $y \in [-11, 11]$. With increasing n, the functions ψ_n spread out from the centre of the integration region and their absolute value goes up.

In numerical calculations, the integration region $x \in [-11, 11]$, $y \in [-11, 11]$ was used. The numerical and analytical ground-state and first excited state perturbation energies are shown in Tables IV–VII.

Only the digits which agree in the calculations for the points $x = [0.2, 0.5]$ and $x = [0.6, 0.8]$ are shown. Dependence of the results on the choice of the point x is small, as in the preceding examples. The numerical results agree with the analytic ones with an accuracy of 6–9 digits.

Because of the antisymmetry of the perturbation potential (32), the odd-order perturbation energies

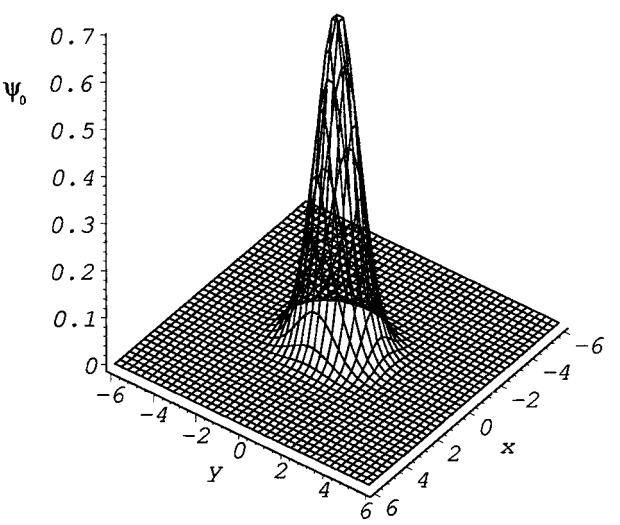

FIGURE 1. Ground-state zero-order wave function ψ_0 for the Hénon–Heiles Hamiltonian (31, 32).

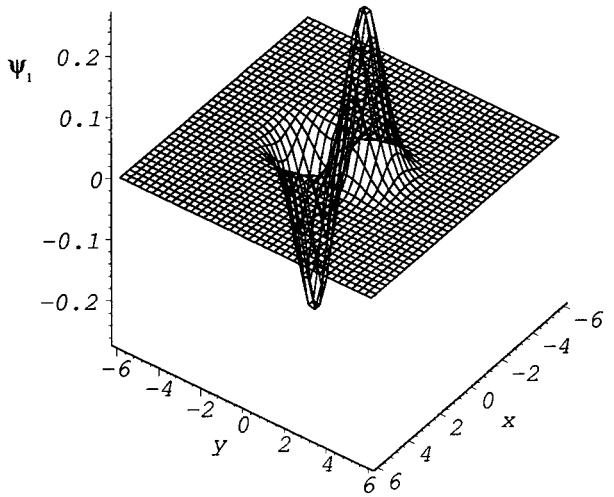

FIGURE 2. First-order perturbation function ψ_1 for the ground state of the Hénon–Heiles Hamiltonian (31, 32).

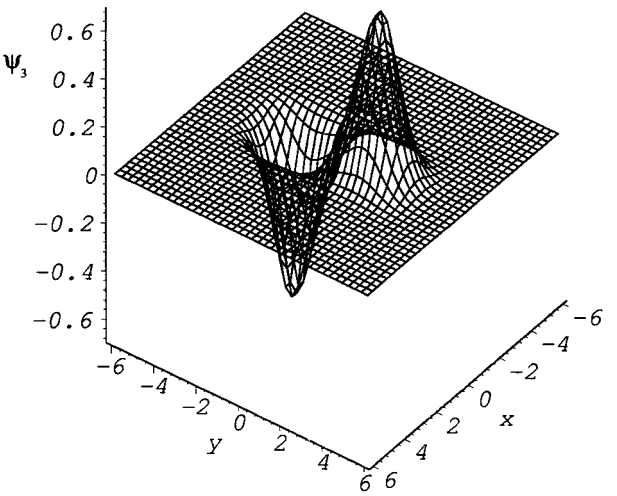

FIGURE 4. Third-order perturbation function ψ_3 for the ground state of the Hénon–Heiles Hamiltonian (31, 32).

E_1, E_3, ... equal zero. In numerical calculations, these energies differ from zero with an accuracy of 7–9 digits. The even-perturbation energies E_2, E_4, ..., are negative, and their absolute value increases rapidly with the order of the perturbation theory.

Results in Tables IV–VII indicate that the absolute values of the perturbation energies E_n increase with the energy difference of the excited state and the ground state.

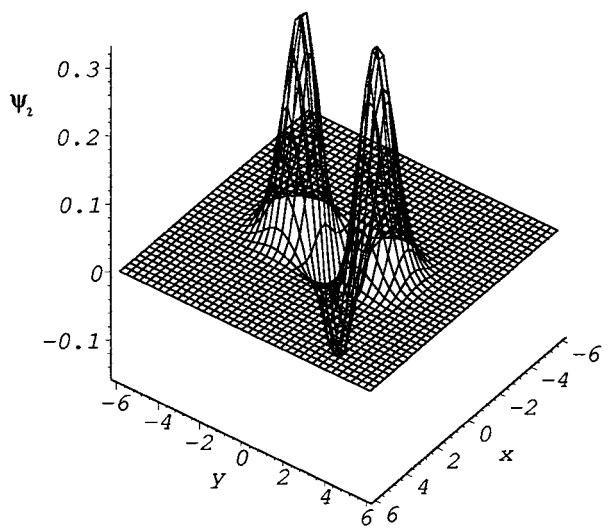

FIGURE 3. Second-order perturbation function ψ_2 for the ground state of the Hénon–Heiles Hamiltonian (31, 32).

Concluding this section, our method of solving the perturbation problem gives good results in the all investigated cases including the most difficult Hénon–Heiles Hamiltonian. The absolute values of the perturbation energies E_n increase rapidly for large n.

4. Conclusions

In summary, the method described in this paper is simple and efficient alternative to the usual formulation of the perturbation theory. It can be used for one-dimensional as well as multidimensional problems and for nondegenerate as well as degenerate eigenvalues. Its main advantages are easy calculation of the large-order perturbations and the possibility to find the perturbation corrections, even in cases when only a few zero-order bound states exist. The analytic and numerical results for the investigated examples show that our version of the perturbation theory yields results with good accuracy and can be used at large orders.

The numerical results show in all investigated examples that the absolute values of the perturbation energies E_n increase rapidly for large n. They also indicate that the perturbation series (4) are divergent, asymptotic series in these cases. They are obviously related to different asymptotic behavior of the wave functions corresponding to the zero-order Hamiltonian $H = H_0$ and the full Hamiltonian $H = H_0 + \lambda H_1$ for $x \to \pm\infty$. Therefore, one should be very careful when truncating such perturbation series at low orders.

TABLE IV

Perturbation energies E_n for the ground state of the Hénon–Heiles Hamiltonian (31, 32); E_0 is the exact zero-order energy.*

n	E_n^{num}	E_n^{an}
0	1.65	$\frac{33}{20} = 1.65$
2	-0.338300661	$-\frac{4096775}{12109864} = -0.338300661345\ldots$
4	-0.95061029	$-\frac{1056557053570119375}{1111451301420501184} = -0.950610298642\ldots$
6	-5.26789699	$-\frac{1316035702524299260768279480015625}{249821836546340968688607521245696} = -5.26789699698\ldots$
8	-41.495774	$-\frac{5846428287938298346999647132258702371673311914062 5}{1408921354549645735897393295254864019710396022784} = -41.4957745445\ldots$
10	-414.584851	$-414.584851968\ldots$
12	-4969.6014	$-4969.60146844\ldots$
14	-69209.077	$-69209.0774461\ldots$
16	-1096653.64	$-1096653.64936\ldots$
18	-0.194809520×10^8	
20	-0.38361825×10^9	
22	$-0.82989680 \times 10^{10}$	
24	$-0.19576261 \times 10^{12}$	
26	$-0.50030730 \times 10^{13}$	
28	$-0.13776229 \times 10^{15}$	
30	$-0.40671279 \times 10^{16}$	

* The energies calculated from Eq. (12) are denoted as E_n^{num}. The analytic energies denoted as E_n^{an} were calculated for $n = 0, 2, \ldots, 16$. For lack of space, the analytic energies E_{10}^{an}, E_{12}^{an}, E_{14}^{an}, and E_{16}^{an} are written as a decimal number only. Odd-order perturbation energies equal zero.

TABLE V

Perturbation energies E_n for the first excited [0, 1] state of the Hénon–Heiles Hamiltonian (31, 32); E_0 is the exact zero-order energy.*

n	E_n^{num}	E_n^{an}
0	2.95	$\frac{59}{20} = 2.95$
2	-2.649761	$-\frac{866382925}{326966328} = 2.64976191982\ldots$
4	-13.663991	$-\frac{298922976349768528158125}{21876695965859724804672} = -13.6639909800\ldots$
6	-130.211814	$-\frac{284303183672173527501751303316806599779 6875}{21833900913142490840925787807662370512384} = -130.211813639\ldots$
8	-1656.04703	$-1656.04702793\ldots$
10	-25297.5508	$-25297.5508014\ldots$
12	-441706.519	$-441706.519216\ldots$
14	-0.85765206×10^7	
16	$-0.1821097391 \times 10^9$	
18	$-0.418283241 \times 10^{10}$	
20	$-0.103158272 \times 10^{12}$	
22	$-0.271740662 \times 10^{13}$	
24	$-0.761625748 \times 10^{14}$	
26	$-0.22644751 \times 10^{16}$	
28	$-0.712486581 \times 10^{17}$	
30	$-0.23673444 \times 10^{19}$	

* The energies calculated from Eq. (12) are denoted as E_n^{num}. The analytic energies denoted as E_n^{an} were calculated for $n = 0, 2, \ldots, 12$. For lack of space, the analytic energies E_8^{an}, E_{10}^{an}, and E_{12}^{an} are written as a decimal number only. Odd-order perturbation energies equal zero.

TABLE VI

Perturbation energies E_n for the second excited [1, 0] state of the Hénon–Heiles Hamiltonian (31, 32); E_0 is the exact zero-order energy.*

n	E_n^{num}	E_n^{an}
0	3.65	$\frac{73}{20} = 3.65$
2	−0.1629972	$-\frac{1973875}{12109864} = -0.162997288821\ldots$
4	−0.403834	$-\frac{448842824539509375}{1111451301420501184} = -0.403834899438\ldots$
6	−2.117584	$-\frac{52901883942516625513219704460937 5}{24982183654634096868607521245696} = -2.11758446234\ldots$
8	−15.76930	$-\frac{73318460327585065113174610057366923047737418164062 5}{46494404700138309284613978743410512650443068751872} = -15.7693083287\ldots$
10	−150.1364	$-150.136468953\ldots$
12	−1730.805	$-1730.80567546\ldots$
14	−23374.8	
16	-0.361673×10^{6}	
18	-0.63081×10^{7}	
20	-0.1224862×10^{9}	
22	-0.262120×10^{10}	
24	-0.613108×10^{11}	
26	-0.155649×10^{13}	
28	-0.426302×10^{14}	
30	$-0.1253085 \times 10^{16}$	

* The energies calculated from Eq. (12) are denoted as E_n^{num}. The analytic energies denoted as E_n^{an} were calculated for $n = 0, 2, \ldots, 12$. For lack of space, the analytic energies E_{10}^{an} and E_{12}^{an} are written as a decimal number only. Odd-order perturbation energies equal zero.

TABLE VII

Perturbation energies E_n for the third excited [1, 1] state of the Hénon–Heiles Hamiltonian (31, 32); E_0 is the exact zero-order energy.*

n	E_n^{num}	E_n^{an}
0	4.95	$\frac{99}{20} = 4.95$
2	−1.845463	$-\frac{201134875}{108988776} = -1.84546411458\ldots$
4	−8.85123	$-\frac{21515087825404789503125}{2430743996206636089408} = -8.85123561303\ldots$
6	−78.03980	$-\frac{69418698706965547421370246418819183882 5125}{88952929646136073796364320697883731717 12} = -78.0398115982\ldots$
8	−919.9970	$-919.997135266\ldots$
10	−13100.3	$-13100.3815465\ldots$
12	−214537.0	$-214537.066115\ldots$
14	-0.3931028×10^{7}	
16	-0.79242×10^{8}	
18	$-0.1737966 \times 10^{10}$	
20	-0.411554×10^{11}	
22	$-0.10463977 \times 10^{13}$	
24	$-0.28444762 \times 10^{14}$	
26	-0.823863×10^{15}	
28	$-0.2535079 \times 10^{17}$	
30	-0.826589×10^{18}	

* The energies calculated from Eq. (12) are denoted as E_n^{num}. The analytic energies denoted as E_n^{an} were calculated for $n = 0, 2, \ldots, 12$. For lack of space, the analytic energies E_{10}^{an} and E_{12}^{an} are written as a decimal number only. Odd-order perturbation energies equal zero.

ACKNOWLEDGMENTS

The authors thank the GA U.K. (grant 166/00), the GA C.R. (grant 202/00/1026), the MS C.R. (grant 100-01/206053) of Czech Republic and NSERC of Canada (J. Z. is a NATO Science Fellow) for support.

References

1. Skála, L.; Čížek, J. J Phys A 1996, 29, L129–L132.
2. Skála, L.; Čížek, J. J Phys A 1996, 29, 6467–6470.
3. Guardiola, R.; Ros, J. J Phys A 1996, 29, 6461–6465.
4. Znojil, M. J Phys A 1996, 29, 5253–5256.
5. Au, C. K.; Chow, C. K.; Chu, C. S. J Phys A 1997, 30, 4133–4136.
6. Skála, L.; Čížek, J.; Zamastil, J. J Phys A 1999, 32, 5715–5734.
7. Skála, L.; Čížek, J.; Kapsa, V.; Weniger, E. J. Phys Rev A 1997, 56, 4471–4479.
8. Skála, L.; Čížek, J.; Weniger, E. J.; Zamastil, J. Phys Rev A 1999, 59, 102–106.
9. Skála, L.; Kalhous, M.; Zamastil, J.; Čížek, J. J Phys A 2002, 35, L167–L174.
10. Vrscay, E. R.; Handy, C. R. J Phys A 1989, 22, 823–834.
11. Banks, T.; Bender, C. M.; Wu, T. T. Phys Rev D 1973, 8, 3346–3466.
12. Monagan, M. B.; Geddes, K. O.; Heal, K. M.; Labahn, G.; Vorkoetter, S. M.; McCarron, J.; DeMarco, P. Maple 9 Introductory Programming Guide, ISBN 1-894511-43-3, Maplesoft, Canada 2003.